Solid-State Electronics Vol. 33, No. 12, pp. 1539–1544, 1990
Printed in Great Britain. All rights reserved

0038-1101/90 $3.00 + 0.00
Copyright © 1990 Pergamon Press plc

ON THE EFFECT OF NON-DEGENERATE DOPING OF POLYSILICON GATE IN THIN OXIDE MOS-DEVICES—ANALYTICAL MODELING

PREDRAG HABAŠ and SIEGFRIED SELBERHERR
Institute for Microelectronics, Technical University Vienna, Gußhausstrasse 27-29,
1040 Vienna, Austria

(Received 20 November 1989; in revised form 4 April 1990)

Abstract—A one-dimensional model of the polysilicon-gate–oxide–bulk structure is presented in order to analyze the implanted gate MOS-devices. The influence of the ionized impurity concentration in the polysilicon-gate near the oxide and the charge at the polysilicon–oxide interface on the flat-band voltage, threshold voltage, inversion layer charge and the quasi-static $C-V$ characteristic is quantitatively studied. The calculations show a considerable degradation of the inversion layer charge due to the voltage drop in the gate, especially in thin oxide devices. The calculated quasi-static $C-V$ curves agree with the recently published data of implanted gate devices.

1. INTRODUCTION

Replacing N^+ with P^+ polysilicon (poly-) gates for P-channel submicron MOS-devices the subthreshold characteristic can be improved because the compensating channel implantation (which leads to buried-channel devices) is avoided[1,2]. In addition, using a refractory-metal–silicide layer over poly-gates significantly lowers the interconnections propagation delay time. Therefore the dopant concentration in poly-gate may be reduced. This allows the poly-gates to be doped by implantation simultaneously with the formation of source and drain, which leads to N^+/P^+-gates for N/P-channel devices, respectively. Due to higher impurity diffusivity along the grain boundaries compared to the single crystal it is possible to dope poly-gates heavily, although their thickness is larger than the source/drain-bulk junctions depth. However, a significant part of the impurities remains non-activated in the grain boundaries after annealing due to segregation[3]. Moreover, if the majority carrier concentration in polysilicon is lower than the equivalent volume trapping states density, the majority carriers are completely trapped in the grain boundaries. The grains are depleted and the polysilicon is highly resistive. Due to these effects the free majority carrier concentration in the poly-gate can be significantly lower than the chemical impurity concentration[4] which depends on doping, grain size and annealing conditions.

It has been experimentally observed that the high-frequency $C-V$ curve of implanted poly-gate devices differs from its degenerate counterpart (shift of the flat-band voltage)[5–7]. The degradation of the quasi-static $C-V$ curve suggests a reduction in the driving capabilities of implanted gate devices in comparison with ones with degenerate gate[5,8,9]. The previous experimental effects have been related to: shift of the Fermi level in poly-gate and depletion in the poly-gate near the oxide (resistive layer) due to penetration of the electric field into the poly-gate or the existence of acceptor type interface traps[5–11]. An additional effect may be boron penetration. It will not be considered in this paper.

Generally, there is a voltage drop in the poly-gate when the gate bias is applied because the electric field is nonzero in the whole polysilicon–oxide–silicon structure. Conventional degenerately doped poly-gates are highly conductive and may be assumed to be equipotential areas. In the case of non-degenerate doping (implantation) the voltage drop in the poly-gate cannot be neglected, especially in thin oxide devices. An analytical modeling of MOS-devices, assuming the poly-gate is a non-equipotential area, has already been proposed in Ref.[10]. The detailed calculations have not been given and the voltage drop in the gate is judged as a secondary effect. The high-frequency $C-V$ curve of the polysilicon–oxide–silicon structure has been discussed theoretically and experimentally in Ref.[6]. In this paper an analytical model of the poly-gate–oxide–silicon structure is given in Section 2. Using it the influence of the ionized impurity concentration in the poly-gate near the oxide, the charge at the poly-gate–oxide interface and oxide thickness on the flat-band voltage, threshold voltage, inversion layer charge and the quasi-static $\tilde{C}-V$ curve is analyzed in Section 3.

2. THE MODEL

The problem is treated one-dimensionally in this paper. Figure 1 shows the N-polysilicon–oxide–P-silicon structure at positive gate bias. The gate–bulk voltage is distributed on poly-gate, oxide and bulk. The basic phenomenological equation, which de-

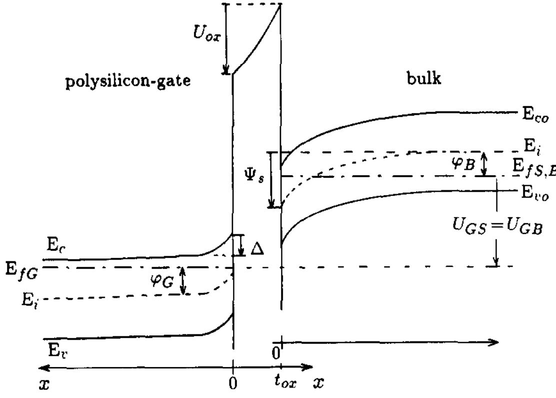

Fig. 1. Band diagram of N-polysilicon–oxide–P-silicon structure at positive gate–source bias. $U_{DS} \approx 0$, $U_{BS} = 0$. The axes for poly-gate, oxide and bulk are shown.

scribes the interaction between poly-gate and bulk, is given by Gauss law

$$E_g(0) = -\frac{\epsilon_s}{\epsilon_g} E_s(0) + \frac{Q_{go} + Q_{os} + Q_{ss}}{\epsilon_g} \quad (1)$$

where $E_g(0)$ is the normal surface field in poly-gate at the gate–oxide interface, $E_s(0)$ is the normal surface field in bulk and ϵ_s, ϵ_g are the permittivities of silicon and polysilicon. Q_{go}, Q_{os} are the surface charges at the gate–oxide and oxide–bulk interfaces, respectively. There is not much information about the nature of Q_{go} in literature[12]. An existence of the electron trapping interface states at the poly–oxide interface has been suggested in Refs[6,7]. A positive Q_{go} (interface trapped + fixed oxide charge) has been experimentally obtained in Ref.[6]. Henceforward, Q_{go} is taken as fixed oxide charge. In eqn (1) Q_{ss} is the total space-charge in the oxide (ρ_{ox} is its density):

$$Q_{ss} = \int_{0+}^{t_{ox}} \rho_{ox}(x)\, dx \quad (2)$$

t_{ox} denotes the oxide thickness. Since $E_s(0)$ is very high in (modern) thin oxide devices, it follows from eqn (1) that $E_g(0)$ is very high too. This leads to a voltage drop in the poly-gate even if it has been heavily doped (Section 3). The potential difference at the oxide is

$$U_{ox} = \frac{\epsilon_s}{C_o} E_s(0) - \frac{Q_{os} + Q_{ss}^e}{C_o} \quad (3)$$

where $C_o = \epsilon_{ox}/t_{ox}$, ϵ_{ox} is the oxide permittivity and Q_{ss}^e is the equivalent charge in the oxide:

$$Q_{ss}^e = \frac{1}{t_{ox}} \int_{0+}^{t_{ox}} x \rho_{ox}(x)\, dx. \quad (4)$$

Note that Q_{ss} differs from Q_{ss}^e. Their ratio depends directly on $\rho_{ox}(x)$. Q_{ss} appears only in eqn (1) and it may be included in the term Q_{go}. An eventual dipole layer in the oxide near the poly–oxide interface, suggested in Ref.[12], leads to an additional term at right-hand side in eqn (3). It is omitted here.

The traps at the grain boundaries will not be taken into account in this paper. We believe such an approach is reasonable for our analysis if the ionized impurity concentration N_G is at least four times larger than the equivalent volume trap density N_{tvol}† [13]. In spite of the rather uniform profile of the chemical concentration of dopant in poly-gates[2,5,14], the profile of the activated impurities can be non-uniform[4]. We approximate the activated impurity profile in poly-gate near the oxide by a constant level N_G. The necessary width of this uniform region is only a few extrinsic Debye length $L_{Dg} = \sqrt{\epsilon_g U_T / e N_G}$. For minimum $N_{Gmin} \sim 5 \times 10^{17}\,\text{cm}^{-3}$ a maximum width $\sim \sqrt{1.2/U_T} \cdot L_{Dg}(N_{Gmin}) \approx 40$ nm is estimated at room temperature, which is much lower than the poly-gate thickness. The remaining part of the poly-gate is in the quasi-neutral condition because of the heavy doping and the real profile is not important.

For the poly-gate a single crystal model including band gap narrowing and Fermi–Dirac (FD) statistics shall be assumed. The Fermi barrier in the poly-gate $\varphi_G = (E_{fG} - E_i)/e$ (Fig. 1) is given by

$$\varphi_G = \frac{E_{co} - E_i}{e} + \phi_{fc} - \frac{\delta E_c}{e} \quad (5)$$

where $\delta E_c = E_{co} - E_c$ is the conduction band shift due to band gap narrowing and ϕ_{fc} is

$$\phi_{fc} = \frac{E_{fG} - E_c}{e} = U_T \cdot F_{1/2}^{-1}\left(\frac{n_o}{N_c}\right); \quad n_o \simeq N_G. \quad (6)$$

In eqn (6) $F_{1/2}^{-1}$ is the inverse Fermi integral of order 1/2 (Appendix A) and n_o is the neutral electron concentration. The surface potential Δ is obtained after integration of Poisson's equation in the homogeneous part of the poly-gate using the condition $E_g(x) \to 0$ for $x \to \infty$. Practically, the field decreases from $E_g(0)$ to a negligible value after a few L_{Dg}. Using FD statistics for both electrons and holes it follows

$$\frac{N_c}{N_G}\left[F_{3/2}\left(\frac{\phi_{fc} - \Delta}{U_T}\right) - F_{3/2}\left(\frac{\phi_{fc}}{U_T}\right)\right] + \frac{\Delta}{U_T}$$
$$+ \frac{N_v}{N_G}\left[F_{3/2}\left(\frac{\phi_{vf} + \Delta}{U_T}\right) - F_{3/2}\left(\frac{\phi_{vf}}{U_T}\right)\right]$$
$$= \frac{1}{2}\left(\frac{E_g(0) L_{Dg}}{U_T}\right)^2 \quad (7)$$

where ϕ_{vf} is

$$\phi_{vf} = \frac{E_v - E_{fG}}{e} = -\frac{E_{go} - \delta E_g}{e} - \phi_{fc} \quad (8)$$

δE_g represents the total band gap narrowing due to heavy doping and $E_{go} = E_{co} - E_{vo}$ is the ideal band gap. The calculation of the Fermi integral $F_{3/2}$ is explained in Appendix A. For $E_g(0) > 0$ follows $\Delta < 0$, while $\Delta > 0$ holds for $E_g(0) < 0$. The three terms at the left-hand side in eqn (7) model the accumulation, depletion and inversion in the N-poly-

†N_{tvol} = grain boundary surface trapping states density/grain size.

gate respectively. In eqns (6, 7) N_c and N_v are the effective density of states for parabolic conduction and valence bands. Using Maxwell–Boltzmann (MB) statistics for both carriers, eqns (5)–(8) reduce to eqns (A.4)–(A.6) given in Appendix A.

The voltage conservation (Fig. 1) using eqn (3) gives

$$U_{GS} = -\varphi_G + \Delta + \frac{\epsilon_s}{C_o} E_s(0) - \frac{Q_{os} + Q_{ss}^e}{C_o} + \Psi_s - \varphi_B. \tag{9}$$

In eqn (9) Ψ_s is the potential of the intrinsic level at surface with respect to the level deep in the bulk, φ_B is the Fermi barrier deep in the bulk. The bulk bias is not taken into account: $U_{BS} = 0$. For a self-consistent solution of the system eqns (1), (7) and (9), it is necessary to know the relationship between $E_s(0)$ and Ψ_s. This relationship depends only on the bulk doping profile. It is given by integration of Poisson's equation in the bulk (e.g.[15]).

3. CALCULATIONS AND DISCUSSION

In order to obtain the quantitative estimates of the effects in poly-gate on the flat-band voltage, threshold voltage and the inversion layer charge, for the sake of simplicity, a uniformly doped bulk is assumed (with doping N_B). For the $\Psi_s \mapsto E_s(0)$ relation an expression analogous to eqn (A.4) (Appendix A) holds. The system eqns (1), (7) or (A.4), (9) and $\Psi_s(E_s(0))$ relation is solved for any U_{GS} using a simple self-consistent iterative approach. For the referential ideal poly-gate $\Delta = 0$ is assumed. Moreover, $\varphi_G = (E_{co} - E_i)/e$ is assumed[4,5,16]. Note that the Fermi level position in degenerately doped polysilicon is not well understood[11,12].

(a) Flat-band voltage

The flat-band voltage has no meaning for a non-homogeneous structure because the flat band condition generally does not exist in the whole structure. We define it by $E_s(0) = 0$[15]. From eqn (9) it follows

$$V_{FB} = -\varphi_G + \Delta^o - \frac{Q_{os} + Q_{ss}^e}{C_o} + \Psi_s^o - \varphi_B \tag{10}$$

where $\Psi_s^o = \Psi_s(E_s(0) = 0)$ is the solution of Poisson's equation. For uniform bulk $\Psi_s^o = 0$ holds. Two terms in eqn (10) contribute to the V_{FB} shift in implanted poly-gate devices: the variation of the equilibrium Fermi level (φ_G) and the surface potential Δ^o due to field $E_g(0)$. The charge at the gate–oxide interface Q_{go} affects V_{FB} only through the term Δ^o. For a common value $Q_{go}/e \sim 10^{12}\,\text{cm}^{-2}$[6], from eqn (1) follows $E_g(0) \sim 150\,\text{kV/cm}$, which produces $\Delta^o \sim -35\,\text{mV}$ for $N_G = 2 \times 10^{18}\,\text{cm}^{-3}$ (accumulation in N-poly-gate). Figure 2 shows $V_{FB} + \varphi_B$ vs N_G for N-poly-gate at different Q_{go} as a parameter. The calculations based on both FD and MB statistics are presented.

For positive Q_{go} the variation of Δ^o with Q_{go} is nearly logarithmic because of the accumulation in

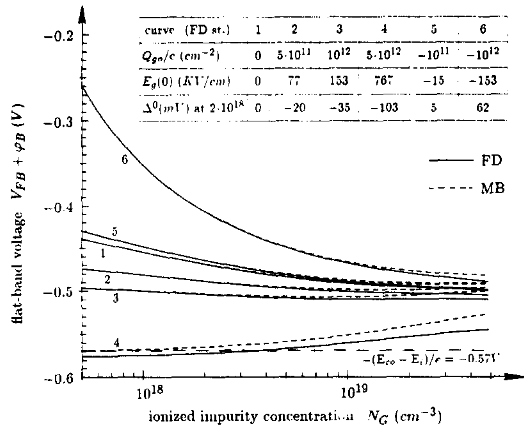

Fig. 2. Flat-band voltage with respect to intrinsic level in the bulk vs ionized impurity concentration in N-poly-gate N_G, with Q_{go} as a parameter.

N-poly-gate. Q_{go} has a low influence on V_{FB}. For negative Q_{go} (which has not been experimentally observed[6]) the influence is higher due to depletion. Note that the positive Q_{go} "improves" V_{FB} (shift towards the degenerate value). Accordingly, the measurement of V_{FB} does not give a reliable proof that a sufficiently high ionized impurity concentration near the oxide is achieved. For P-poly-gates a positive Q_{go} can produce a significant Δ^o due to depletion. For example: at $N_G = 2 \times 10^{18}\,\text{cm}^{-3}$ for $Q_{go}/e = 10^{12}\,\text{cm}^{-2}$ follows $\Delta^o = -62\,\text{mV}$, while $Q_{go}/e = 5 \times 10^{12}\,\text{cm}^{-2}$ leads to $\Delta^o = -950\,\text{mV}$ (onset of inversion in poly-gate). Measuring V_{FB} at different t_{ox}, the charge in the oxide may be extracted from V_{FB} using the well known extrapolation technique[11,12,17]. In our case such a technique gives a value of Q_{os} and $-\varphi_G + \Delta^o$ (assuming $\rho_{ox} = 0$). Both terms φ_G and Δ^o depend on the unknown N_G. Moreover, Δ^o depends on Q_{go} also. Consequently, a proper extraction of Q_{go} and N_G from V_{FB} data is not possible. In Fig. 2 moderate doping is taken into consideration. V_{FB} is a weak function of N_G. It is close to the degenerate value $\sim -0.52\,\text{V} - \varphi_B$. At low doping, for $N_G < N_{tvol}$, the grains in poly-gate are depleted due to trapping at grain boundaries and the Fermi level in N-poly-gate is shifted downwards (in P-poly-gate upwards). This (rapid) variation of φ_G with decrease of doping causes a shift of V_{FB}, which depends on the energy level and density of the trapping states in grain boundaries. The considerable changes of V_{FB}[2,5] and U_t[1] for a low implant dose and/or annealing temperature can be related to this effect.

The calculations show clearly the small differences between results obtained by FD and MB statistics. The contribution of the second term in eqn (A.1) (correction due to FD statistics) to φ_G is only 9 mV, 15 mV for N,P-poly-gates at doping $5 \times 10^{19}\,\text{cm}^{-3}$. Actually, the impact of FD statistics on our calculations is less than the uncertainness of the model eqn (A.3) for the band gap narrowing. For doping

higher than $5 \times 10^{19}\,\text{cm}^{-3}$ the differences between FD and MB statistics become significant but the poly-gates may then be assumed to be degenerate.

(b) Threshold voltage

From eqn (9) the threshold voltage follows

$$U_t = -\varphi_G + \Delta^t - \frac{Q_{os} + Q_{ss}^t}{C_o} + \frac{\epsilon_s}{C_o} E_s^t(0) + \Psi_s^t - \varphi_B \tag{11}$$

where "t" denotes the value at threshold. The last four terms at the right-hand side in eqn (11) do not depend on poly-gate. In thin oxide devices the necessary field to produce the inversion $E_s^t(0)$ is very high. Consequently, the field $E_g(0)$ is very high too and the surface potential Δ^t cannot be neglected. In Fig. 3 U_t and Δ^t against N_G are given, with t_{ox} and Q_{go} as parameters.

The calculations show that both factors Δ^t and the difference of φ_G from its degenerate value are of the same order. The term Δ^t is considerably emphasized for thin oxides (curve 1), because of the high corresponding $E_s^t(0)$. For thick oxides the term Δ^t becomes less important (curve 3). The positive charge at the gate–oxide interface Q_{go} lowers the field $E_g(0)$ (eqn (1)), and therefore it reduces Δ^t. For common values of Q_{go}[6] this "screening" effect is rather pronounced. Therefore, the positive Q_{go} reduces the variation of U_t with N_G in N-channel devices. An eventual negative Q_{go} has opposite influence. In P-channel devices (P-poly-gate) the positive fixed change Q_{go} increases the field $E_g(0)$ and therefore increases the variation of U_t with N_G.

(c) Inversion layer charge and capacitances

The surface field $E_s(0)$ is very high in strong inversion in thin oxide devices, even at medium gate bias (for example $U_{ox} = 2\,\text{V}$, $t_{ox} = 8\,\text{nm}$, $E_s(0) \sim 800\,\text{kV/cm}$). Since the field $E_g(0)$ is very high too, the produced voltage drop Δ can lower significantly the effective gate bias (eqn (9)). The inversion layer charge Q_i and finally the drain current can be reduced, leading to degradation of the driving capabilities of devices and the speed of circuit. Figure 4 shows Q_i against U_{GS} with N_G and Q_{go} as parameters. Q_i is calculated as

$$\epsilon_s E_s(0) - \sqrt{2e\epsilon_s N_B}\sqrt{\Psi_s - U_T}.$$

A thin oxide is assumed (8 nm). The calculations show a significant reduction in Q_i, even for a high N_G ($10^{19}\,\text{cm}^{-3}$). Note that for $N_G = 10^{19}\,\text{cm}^{-3}$ the differences of V_{FB} and U_t from their degenerate counterparts are very small (Figs 2 and 3). A doping $N_G \geqslant 4 \times 10^{19}\,\text{cm}^{-3}$ is necessary to obtain a negligible voltage drop in the poly-gate at the highest operating gate bias. The reduction of $E_g(0)$, due to the "screening" effect, is small for common values of Q_{go}. N_G is the basic parameter which determines the degradation of Q_i in strong inversion for a given t_{ox}. The quasi-static C–V curves corresponding to Fig. 4 are given in Fig. 5. The calculation of the total quasi-static capacitance of the polysilicon–oxide–silicon structure C_{tot} is explained in Appendix B. For negative gate voltages a small reduction in C_{tot} occurs due to accumulation in the poly-gate. For positive gate bias, at first a significant decrease of C_{tot} occurs, which can be related to the depletion in poly-gate. This decrease depends directly on N_G and it is figure of merit of Q_i and drain current degradation. A sharp recovery to the ideal C–V at positive bias is caused by the inversion in poly-gate near gate–oxide interface (points A, B). In Fig. 4 the inversion is manifested as a change of the $Q_i(U_{GS})$ slope (the recovery of g_m occurs). In spite of high N_G, for thin oxides the

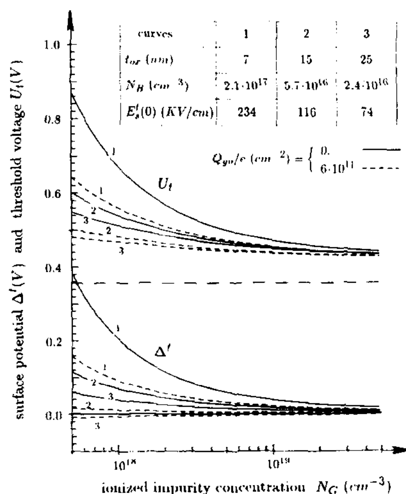

Fig. 3. Surface potential Δ^t (voltage drop in poly-gate) and threshold voltage vs ionized impurity concentration in N-poly-gate N_G, with Q_{go} and t_{ox} as parameters. A homogeneous bulk is assumed. The same ideal threshold voltage $\approx 0.36\,\text{V}$ corresponds to each curve. FD statistics is assumed.

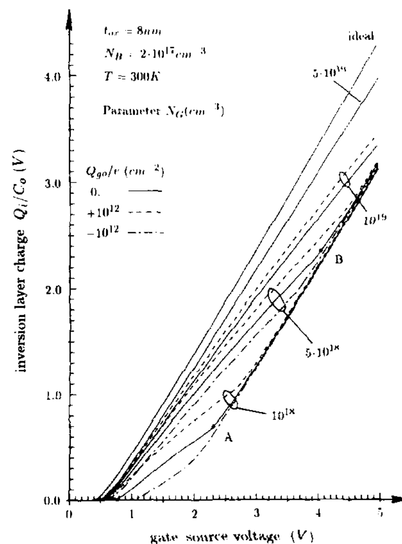

Fig. 4. Inversion layer charge against gate–source bias with N_G and Q_{go} as parameters. The points A, B denote the inversion in poly-gate. FD statistics is assumed.

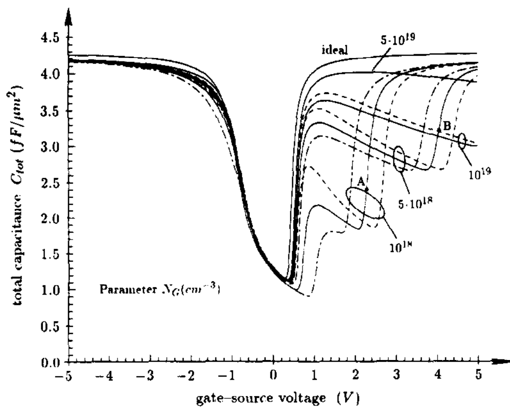

Fig. 5. Quasi-static C–V curves corresponding to Fig. 4.

inversion in poly-gate arises at medium gate bias (for point B: $U_{GS} = 4.04$ V, $U_{ox} = 2.96$ V, $E_g(0) = 1.22$ MV/cm, $\Delta = 0.97$V). For a lower N_G the recovery of C_{tot} to ideal value occurs at a lower U_{GS}. Figure 5 is in qualitative agreement with Fig. 1 from paper[9]. A comparison between the presented model and the experimental C–V data is shown in Fig. 6. Our calculations predict the decrease of C_{tot} due to depletion and the U_{GS} bias at which the inversion in poly-gate occurs. The good agreement with the quasi-static C–V curves given in Ref.[5] is obtained too.

4. CONCLUSION

A system of equations for the one-dimensional analysis of the poly-gate–oxide–bulk structure is formulated and discussed. The band gap narrowing and Fermi–Dirac statistics in the poly-gate are taken into account. However, it has been shown that the assumption of Maxwell–Boltzmann statistics in the poly-gate is reasonable for the analysis performed. Comparing with the conventional model of MOS-devices, there are two new parameters in our analysis: the activated doping concentrations in the poly-gate near the oxide N_G and the surface charge at the gate–oxide interface Q_{go}. The impact of Q_{go} on the flat-band and threshold voltage is judged as strong. Assuming a positive fixed charge Q_{go} this is particularly true for P-gates. Note, that the chemical concentration of impurities is usually lower in P-gates than in N-gates[5] (a limited solubility of boron in poly-gates has been reported[14]). However, contrary to N-gates, the activation is very high in P-gates due to absence of boron segregation at grain boundaries[3]. The calculations presented in this paper are valid if $N_G > N_{tvol}$. A typical value $N_{tvol} \sim 10^{17} \div 10^{18}$ cm^{-3} has been evaluated in the literature (Refs[3,6,13] and references within). If N_G exceeds such a value the flat-band voltage, and the threshold voltage become close to degenerate value. In order to achieve the maximum performances of devices the degradation of the inversion layer charge Q_i must be negligible in the whole operating region. This is assured by N_G considerably higher than for V_{FB} and U_t especially in the case of thin oxide devices. Finally, we believe both V_{FB} and U_t are not the sufficiently proper indicators of the activated doping concentration in the poly-gate near the oxide. It is necessary to take the whole quasi-static C–V characteristic in order to proof the achieved performance of the implanted gate devices. Note finally that the dopant concentration-dependent permittivity, assumed in Ref.[18], has not been taken into account in this paper. This effect has been reported at very low temperature[19,20] where a large amount of non-ionized impurities exists. We speculate it can be important in modeling of the space-charge regions in heavily doped silicon at room temperature too, because of the non-complete activation of impurities.

Acknowledgements—We have pleasure to thank Professor H. Pötzl for many critical and stimulating discussions. Our work is considerably supported by the research laboratories of Digital Equipment Corporation at Hudson, U.S.A.

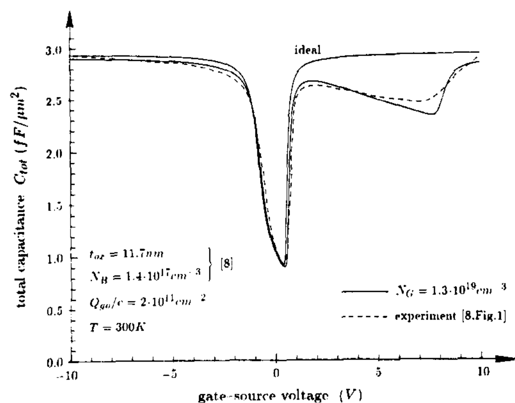

Fig. 6. Comparison between model and experiment (Fig. 1 from paper[8]). A typical value of Q_{go} is assumed. Other parameters are taken from Ref.[8].

REFERENCES

1. J. R. Pfiester and L. C. Parrillo, *IEEE Trans. Electron Devices* **35,** 1305 (1988).
2. S. Nygren, D. T. Amm, D. Levy, J. Torres, G. Göltz, T. T. D'ouville and Ph. Delpech, *IEEE Trans. Electron Devices* **ED-36,** 1087 (1989).
3. M. M. Mandurah, K. C. Saraswat and C. R. Helms, *J. appl. Phys.* **51,** 5755 (1980).
4. J. Y.-C. Sun, R. Angelucci, C. Y. Wong, G. Scilla and E. Landi, *J. Phys.* **C4,** 401 (1988).
5. C. Y. Wong, J. Y.-C. Sun, Y. Taur, C. S. Oh, R. Angelucci and B. Davari, *IEDM Tech. Dig.*, p. 238 (1988).
6. G. Yaron and D. Frohman-Bentchkowsky, *Solid-St. Electron.* **23,** 433 (1980).
7. N. Lifshitz and S. Luryi, *IEEE Trans. Electron Devices* **ED-30,** 833 (1983).
8. R. A. Chapman, C. C. Wei, D. A. Bell, S. Aur, G. A. Brown and R. A. Haken, *IEDM Tech. Dig.*, p. 52 (1988).
9. C.-Y. Lu, J. M. Sung, H. C. Kirsch, S. J. Hillenius, T. E. Smith and L. Manchanda, *IEEE Electron Device Lett.* **10,** 192 (1989).

10. A. H. Marshak and R. Shrivastava, *Solid-St. Electron.* **26**, 361 (1983).
11. N. Lifshitz, *IEEE Trans. Electron Devices* **ED-32**, 617 (1985).
12. T. W. Hickmott and R. D. Isaac, *J. appl. Phys.* **52**, 3464 (1981).
13. A. F. M. Anwar and A. N. Khondker, *IEEE Trans. Electron Devices* **ED-34**, 1323 (1987).
14. U. Schwalke, C. Mazure and F. Neppl, *Mat. Res. Soc. Symp. Proc.* **106**, 187 (1988).
15. F. Van de Wiele, *Solid-St. Electron.* **27**, 824 (1984).
16. D. Peters, *IEEE Trans. Electron Devices* **ED-33**, 1391 (1986).
17. A. S. Grove, *Physics and Technology of Semiconductor Devices*. Wiley, New York (1967).
18. K. W. Teng and S. S. Li, *Solid-St. Electron.* **28**, 277 (1985).
19. T. G. Castner, N. K. Lee, G. S. Cieloszyk and G. L. Salinger, *Phys. Rev. Lett.* **34**, 1627 (1975).
20. S. Dhar and A. H. Marshak, *Solid-St. Electron.* **28**, 763 (1985).
21. N. G. Nilsson, *Appl. Phys. Lett.* **33**, 653 (1978).
22. S. N. Mohammad, *Solid-St. Electron.* **30**, 713 (1987).
23. X. Aymerich-Humet, F. Serra-Mestres and J. Millán, *Solid-St. Electron.* **24**, 981 (1981).
24. D. S. Lee and J. G. Fossum, *IEEE Trans. Electron Devices* **ED-30**, 626 (1983).

APPENDIX A

Heavy Doping Effects and Approximation by Maxwell–Boltzmann Statistics

The inverse Fermi integral of order 1/2 is calculated using Nilsson's expression[21]

$$F_{1/2}^{-1}(x) \simeq \ln x + \frac{x}{[64 + 0.05524\, x\, (64 + \sqrt{x})]^{1/4}}. \quad \text{(A.1)}$$

For other approaches see for example[21,22]. Fermi integrals (Γ is gamma function)

$$F_i(x) = \frac{1}{\Gamma(i+1)} \int_0^\infty \frac{t^i}{1 + \exp(t - x)}\, dt \quad \text{(A.2)}$$

of order i = 1/2 and i = 3/2 are calculated using the approximations proposed by Aymerich-Humet *et al.* in Ref.[23]. Band gap narrowing is described by[22]

$$\delta E_g = 64.76 \cdot \ln\left(\frac{N_G(\mathrm{cm}^{-3}) + 6.73 \times 10^{18}}{10^{20}}\right) + 191\ \mathrm{meV} \quad \text{(A.3)}$$

which agrees with quite scattered experimental data for the electrical energy gap narrowing in literature[24]. We assume $\delta E_c = \delta E_g/2$ in our calculations.

For N-poly-gates the term $F_{3/2}(\phi_{vf}/U_T)$ in eqn (7) may be well approximated using MB statistics. We believe it is reasonable to use MB statistics for both electrons and holes in modeling of poly-gate for doping less than $5 \times 10^{19}\ \mathrm{cm}^{-3} \sim N_c, N_v$. Equation (7) reduces then to

$$\exp(-\Delta/U_T) - 1 + \frac{\Delta}{U_T} + \exp[(\Delta - 2\varphi_{Ge})/U_T] = \frac{1}{2}\left(\frac{E_g(0)L_{Dg}}{U_T}\right)^2 \quad \text{(A.4)}$$

where φ_{Ge} is the effective Fermi barrier

$$\varphi_{Ge} = U_T \ln \frac{N_G}{n_{ie}}; \quad n_{ie} = n_{io} \cdot \exp(\delta E_g / 2eU_T). \quad \text{(A.5)}$$

In eqn (A.5) n_{io} and n_{ie} are "pure" and effective intrinsic concentrations in poly-gate. Fermi barrier φ_G is given as

$$\varphi_G = \varphi_{Ge} - \frac{\delta E_c - \delta E_v}{2e}. \quad \text{(A.6)}$$

Using MB statistics from eqn (B.3) poly-gate capacitance follows

$$C_g = \frac{eN_G}{-E_g(0)} \{1 - \exp(-\Delta/U_T) + \exp[(\Delta - 2\varphi_{Ge})/U_T]\}. \quad \text{(A.7)}$$

For $E_g(0) = 0$ the flat-band capacitance $C_g = \epsilon_g / L_{Dg}$ holds.

APPENDIX B

Calculation of the Capacitances

The total capacitance of the polysilicon–oxide–silicon structure is defined by

$$C_{tot} = \frac{-\partial Q_s}{\partial U_{GB}} = \frac{\partial Q_g}{\partial U_{GB}} \quad \text{(B.1)}$$

where Q_s, Q_g are induced charge in the bulk and poly-gate respectively. Q_{go}, Q_{os} are assumed to be fixed oxide charge. Differentiating eqn (9) with respect to U_{GS} ($= U_{GB}$), using $Q_s = -\epsilon_s E_s(0)$, after simple transformations it follows

$$C_{tot} = \left(\frac{1}{C_g} + \frac{1}{C_o} + \frac{1}{C_s}\right)^{-1} \quad \text{(B.2)}$$

$C_s = -\partial Q_s / \partial \Psi_s$ and $C_g = \partial Q_g / \partial \Delta$ are the bulk and gate capacitances respectively. Differentiating eqn (7), using $Q_g = -\epsilon_g E_g(0)$, yields

$$C_g = \frac{eN_G}{-E_g(0)} \left[1 - \frac{N_c}{N_G} F_{1/2}\left(\frac{\phi_{fc} - \Delta}{U_T}\right) + \frac{N_v}{N_G} F_{1/2}\left(\frac{\phi_{vf} + \Delta}{U_T}\right)\right]. \quad \text{(B.3)}$$

For $E_g(0) = 0$ the derivation leads to the flat-band capacitance given by $F_{-1/2}$ integrals. For C_s an expression analogous to solely (A.7) may be written. Note that the ideal C_{tot} is obtained from eqn (B.2) by $C_g \to \infty$. The corresponding C_s is calculated using Ψ_s and $E_s(0)$ calculated from eqn (9) and Ψ_s, $[E_s(0)]$ relation with $\varphi_G = (E_{co} - E_i)/e$ and $\Delta = 0$.